Detection of a Hard Tail in the X-ray Spectrum of the Z Source GX 349+2

T. Di Salvo[1,2], N. R. Robba[1], R. Iaria[1], L. Stella[3,4], L. Burderi[3], G. L. Israel[3,4]

ABSTRACT

We present the results of a BeppoSAX observation of the Z source GX 349+2 covering the energy range 0.1–200 keV. The presence of flares in the light curve indicates that the source was in the flaring branch during the BeppoSAX observation. We accumulated energy spectra separately for the non-flaring intervals and the flares. In both cases the continuum is well described by a soft blackbody ($kT_{\rm BB} \sim 0.5$ keV) and a Comptonized spectrum corresponding to an electron temperature of $kT_{\rm e} \sim 2.7$ keV, optical depth $\tau \sim 10$ (for a spherical geometry), and seed photon temperature of $kT_{\rm W} \sim 1$ keV. All temperatures tend to increase during the flares. In the non-flaring emission a hard tail dominates the spectrum above 30 keV. This can be fit by a power law with photon index ~ 2, contributing $\sim 2\%$ of the total source luminosity over the BeppoSAX energy range. A comparison with hard tails detected in some soft states of black hole binaries suggests that a similar mechanism could originate these components in black hole and neutron star systems.

Subject headings: accretion discs – stars: individual: GX 349+2 — stars: neutron stars — X-ray: stars — X-ray: spectrum — X-ray: general

1. Introduction

Low Mass X-ray Binaries (LMXB) are usually divided into Z and Atoll sources, according to the path they describe in a X-ray Color-Color Diagram (CD) or hardness-intensity diagram (Hasinger & van der Klis 1989). The six known Z sources in the Galaxy are among the most luminous LMXBs and close to the Eddington limit ($L_{\rm Edd}$) for a 1.4 $M_\odot$ neutron star (NS). The instantaneous position of an individual source in the CD is an indicator of the mass accretion rate (e.g. Hasinger et al. 1990), which most likely increases along the Z track from the top left to the bottom right.

[1]Dipartimento di Scienze Fisiche ed Astronomiche, Università di Palermo, via Archirafi n.36, 90123 Palermo, Italy; disalvo@gifco.fisica.unipa.it.

[2]Astronomical Institute "Anton Pannekoek," University of Amsterdam and Center for High-Energy Astrophysics, Kruislaan 403, NL 1098 SJ Amsterdam, the Netherlands.

[3]Osservatorio Astronomico di Roma, Via Frascati 33, 00040 Monteporzio Catone (Roma), Italy; stella@coma.mporzio.astro.it.

[4]Affiliated with the International Center for Relativistic Astrophysics.

The LMXBs of the Atoll class usually have lower luminosities than Z sources (generally in the range 0.01–0.1 $L_{\rm Edd}$). These sources can be found in soft or hard states (see Barret et al. 2000). In the hard state their spectrum is dominated at high energies by a power law, sometimes showing an exponential cutoff at energies of $\gtrsim 100$ keV (see e.g. Barret et al. 2000, and references therein). On the other hand, the spectrum of the Z sources is much softer, with cutoff energies usually well below 10 keV. However, hard tails were occasionally detected in their spectra. The first detection was in the spectrum of Sco X–1; beside the main X–ray component, at a temperature of ~ 4 keV, Peterson & Jacobson (1966) found a hard component dominating the spectrum above 40 keV. The latter component was observed to vary as much as a factor of 3. Since then hard tails were repeatedly searched for in the spectrum of Sco X–1 and other Z sources: they were detected on occasions (e.g. Buselli et al. 1968; Riegler, Boldt, & Serlemitsos 1970; Agrawal et al. 1971; Haymes et al. 1972), but in most cases they were not found, perhaps due to pronounced variations (e.g. Miyamoto & Matsuoka 1977, and references therein; Soong & Rothschild 1983; Jain et al. 1984; Ubertini et al. 1992). Recently a hard tail was detected in another Z source, GX 17+2, observed by BeppoSAX in a broad energy range (0.1–200 keV). In this case the intensity variations of the hard tail were clearly correlated with the source spectral state: a factor of 20 decrease was observed moving from the Horizontal Branch (HB) to the Normal Branch (NB; Di Salvo et al. 2000). The presence of a variable hard tail in Sco X–1 was confirmed by OSSE and RXTE observations (Strickman & Barret 2000; D'Amico et al. 2000). A hard tail was also detected in Cir X–1 (Iaria et al. 2001) and in type-II bursts from the Rapid Burster (Masetti et al. 2000).

GX 349+2, also known as Sco X–2, is one of the six Z sources. Similar to the case of Sco X–1, GX 349+2 possesses a short and underdeveloped HB (if at all). The source variability in the frequency range below 100 Hz is closely correlated with the source position on the X-ray CD, as in other Z sources. Twin quasi periodic oscillations at kHz frequencies (kHz QPO) were detected in the upper and middle NB (Zhang, Strohmayer, & Swank 1998). In this paper we report the results of a spectral study of GX 349+2 in the energy range 0.1–200 keV based on data obtained with BeppoSAX. This led to the detection of a hard component, fitted by a power law with photon index ~ 1.8 or by a thermal bremsstrahlung with $kT \sim 120$ keV.

2. Observations and Analysis

The Narrow Field Instruments (NFI) on board BeppoSAX satellite are four co-aligned instruments which cover more than three decades in energy, from 0.1 keV up to 200 keV, with good spectral resolution over the whole range (see Boella et al. 1997a for detailed description of BeppoSAX instruments). These are two Medium Energy Concentrator Spectrometers, MECS (position sensitive proportional counters operating in the 1.3–10 keV band, Boella et al. 1997b), a Low Energy Concentrator Spectrometer, LECS (a thin window position sensitive proportional counter with extended low energy response, 0.1–10 keV; Parmar et al. 1997), a High Pressure Gas Scintillation Proportional Counter (HPGSPC; energy range of 7–60 keV; Manzo et al. 1997) and a Phoswich

Detection System (PDS; energy range of 13–200 keV; Frontera et al. 1997).

GX 349+2 was observed by BeppoSAX from 2000 March 10 20:42 UT to March 11 23:10 UT, with an effective exposure time of $\sim$ 16 ks in the LECS, $\sim$ 45 ks in the MECS, $\sim$ 45 ks in the HPGSPC, and $\sim$ 22 ks in the PDS. We selected the data for scientific analysis in circular regions centered on the source with $8'$ and $4'$ radius for LECS and MECS, respectively. The background subtraction was obtained with standard methods by using blank sky observations. The background subtraction for the high-energy (non-imaging) instruments was obtained by using off-source data for the PDS and Earth occultation data for the HPGSPC. There is no evidence indicating the presence of contaminating sources in the FOVs of the HPGSPC and PDS, either in the on-source and off-source positions. In fact the off-source PDS count rates are in the expected range and the HPGSPC and PDS spectra align well with each other and the MECS spectra.

Relative normalizations of the four NFIs were treated as free parameters in the model fitting, except for the MECS normalization that was fixed to a value of 1. We checked after the fitting procedure that these normalizations were in the standard range for each instrument[5]. The energy ranges used in the spectral analysis were: 0.12–4 keV for the LECS, 1.8–10 keV for the MECS, 8–40 keV for the HPGSPC, and 15–200 keV for the PDS. We rebinned the energy spectra in order to have approximately the same number of bins per instrument resolution element across the entire energy range. Moreover a 1% systematic error was applied to all these spectra in order to take into account calibration residuals.

In Figure 1 we show the 200 s binned MECS light curve of GX 349+2 in the 1.8–10 keV range. A flare, lasting $\sim$ 4 ks, is clearly apparent close to the beginning of the observation, followed by a series of smaller flares. In Figure 2a we show the CD of GX 349+2, where we defined the Hard Color (HC) as the ratio of the counts in the 7–10.5 keV to the 4.5–7 keV energy bands, and the Soft Color (SC) as the ratio of the counts in the 4.5–7 keV to the 1.8–4.5 keV bands. The SC and HC relationship versus the source intensity in the 1.8–10.5 keV is also shown in Figure 2b (upper and lower panel, respectively). The color variations in these diagrams are mainly due to the spectral changes associated with the flares, during which both the HC and the SC increase. In consideration of presence of fairly large flares in the light curve and the shape of the source variations in the CD, we identify the state of the source with the flaring branch (FB) of the Z path. Hints of the NB/FB vertex are visible in the diagrams at $SC \sim 0.2$ and $HC \sim 0.3$. We extracted energy spectra during the non-flaring intervals, corresponding to SC lower than 0.48, and during the flares, corresponding to SC higher than 0.48.

We tried several two-component models to fit the source X-ray spectrum during the non-flaring state. In particular we tried a blackbody or a disk multicolor blackbody (`diskbb` in XSPEC, Mitsuda et al. 1984) to describe the softer component, and blackbody or Comptonization models such as a power law with high energy exponential cutoff, `compst` (Sunyaev & Titarchuk 1980),

[5]See the BeppoSAX handbook at http://www.sdc.asi.it/software/index.html.

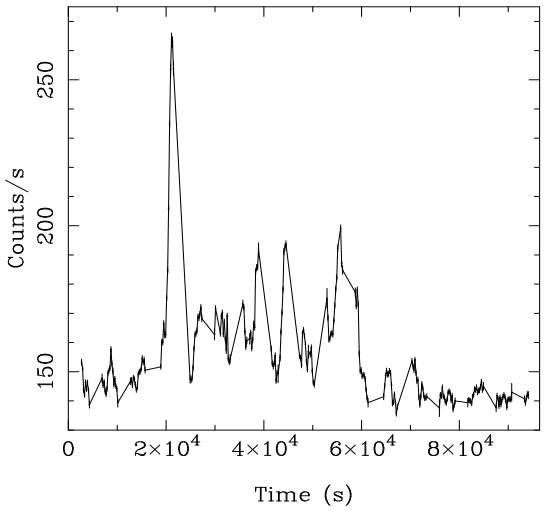

Fig. 1.— Light curve of GX 349+2 in the 1.8–10 keV (MECS data). Each bin corresponds to 200 s integration time.

`comptt` (Titarchuk, 1994), and `pexriv` (*i.e.* a power law with exponential cutoff with its reflection component, Magdziarz & Zdziarski 1995) to describe the harder component. None of these models could well describe the source X-ray spectrum in the whole BeppoSAX energy range, because an excess of emission was present above $\sim$ 30 keV (see Fig. 3a, upper and middle panels). We then considered the low energy part (0.1–30 keV) of the spectrum, where we obtained the best fit by using a blackbody plus `comptt` for the continuum: this model gave a reduced chisquare of $\chi^2_{\rm r} = 1.19$, while we obtained $\chi^2_{\rm r}$ from 1.49 to 2.35 for the other models we fitted. An emission line at $\sim$ 6.7 keV and an edge at $\sim$ 8.5 keV, probably produced by highly ionized iron, are also necessary (probability of chance improvement of the fit $< 10^{-20}$ and $\sim 8.6 \times 10^{-5}$ for the addition of an emission line and an absorption edge, respectively). The fit is further improved by the addition of a low energy Gaussian emission line at $\sim$ 1.16 keV (chance probability of $\sim 7 \times 10^{-9}$).

A two-component continuum model was not sufficient to well fit the non-flaring spectrum in the whole BeppoSAX range. A hard excess is clearly visible above 30 keV with respect to any of the two-component models that we tried. For example, the best fit model described above, when fitted in the whole 0.1–200 keV range, gives rise to the residuals (in units of σ) shown in Figure 3a (middle panel). A significant improvement of the fit was obtained by adding to the model a power law with photon index $\sim$ 1.9, which eliminates the residuals at high energies (see Fig. 3b,

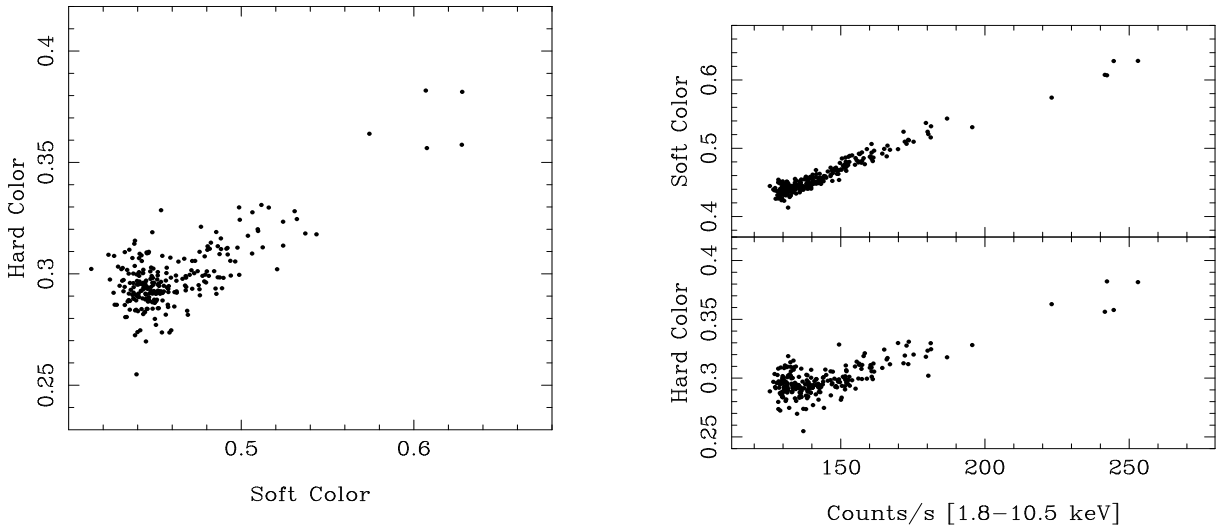

Fig. 2.— a) Color-Color Diagram of GX 349+2. The Hard Color is the ratio of the counts in the 7–10.5 keV and the 4.5–7 keV energy bands, and the Soft Color is the ratio of the counts in the 4.5–7 keV and 1.8–4.5 keV energy bands. Each bin corresponds to 200 s. b) Soft Color (upper panel) and Hard Color (lower panel) versus the source count rate in the MECS (energy range 1.8–10.5 keV).

lower panel). With the addition of this component the χ^2 decreases from 397 (for 191 d.o.f) to 220 (189 d.o.f.). An F-test indicates that the probability of chance improvement is negligibly small. The contribution of this power law component to the unabsorbed 0.1-200 keV luminosity is $\sim 2\%$. Alternative models for the hard excess cannot be excluded. Using a thermal bremsstrahlung for the hard component we obtain a similarly good fit for a temperature of $kT_{\rm TB} = 120 \pm 50$ keV. A high energy power-law spectrum might in principle be produced by Comptonization of seed photons with a blackbody distribution in a optically thin, hot region. Therefore we also tried to fit the hard component using the Comptonization model `compbb` (Nishimura, Mitsuda, & Itoh 1986), which, however, gave a worse fit. In particular we substituted the blackbody plus power law of the best fit model with `compbb`, obtaining a $\chi^2_r = 1.41$ (for 189 d.o.f.) and a temperature of the optically thin Comptonizing region higher than 150 keV. The high χ^2_r is due to large residuals (up to $4-5\ \sigma$) in the energy range above ~ 70 keV, because of a sharp cutoff in the model, which is not present in the data. In other words, because these data do not show a high energy cutoff in the BeppoSAX

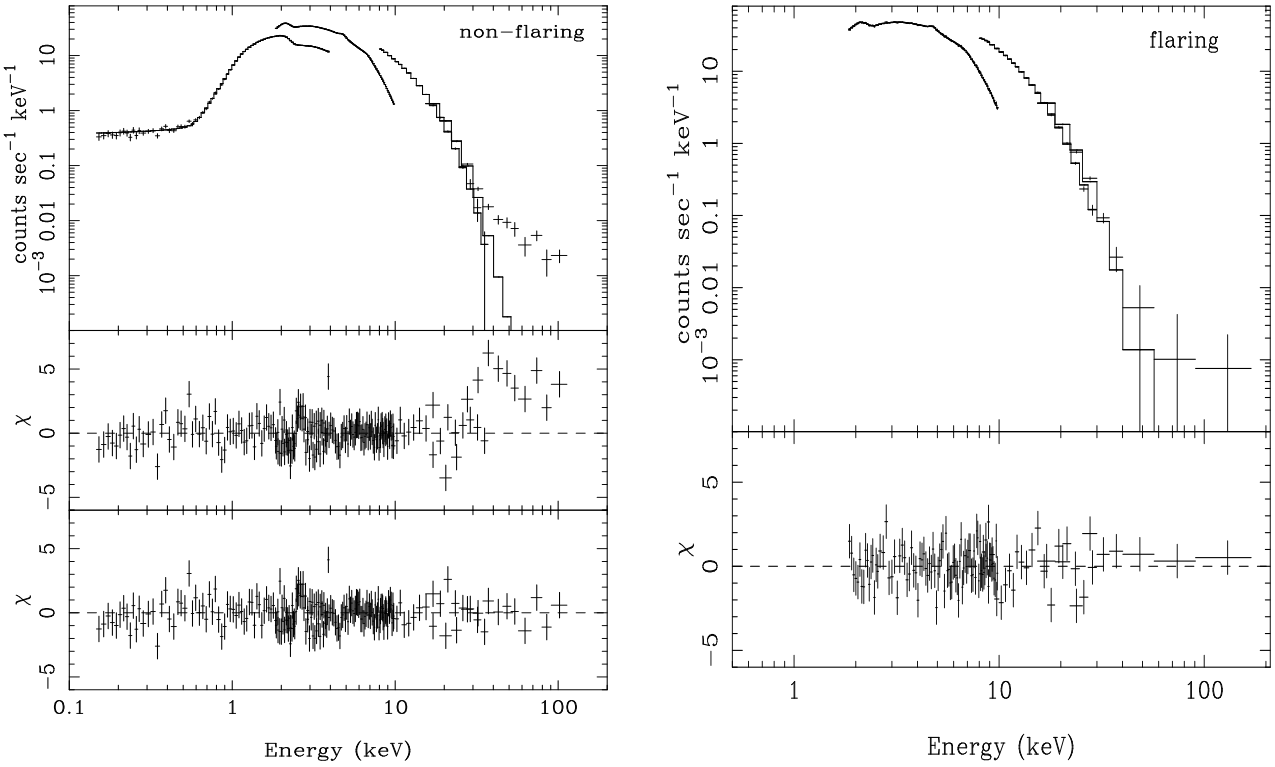

Fig. 3.— a) Broad band spectrum of GX 349+2 during the non-flaring emission together with the best fit two-component continuum model (blackbody plus `comptt`, upper panel), and the corresponding residuals in unit of σ (middle panel). Residuals in unit of σ (lower panel) with respect to the best fit model reported in Table 1, including a power-law hard component. b) GX 349+2 spectrum during flaring intervals together with the best fit model (upper panel), and residuals in unit of σ (lower panel).

range, this implies a high electron temperature ($\gtrsim$ 100 keV) or a non-thermal origin.

No useful LECS data were obtained during the flares, because of the low exposure time: due to UV contamination problems, the LECS is usually operated only at satellite night time, resulting in a much reduced on-source time; therefore low energy data (0.1–1.8 keV) were not available in this case. The spectrum during the flare cannot be described by a single component, such as a blackbody or a `comptt`. As in the case of the non-flaring spectrum, we obtained a good fit using a blackbody plus `comptt` model. The addition of an iron line, with centroid energy and width fixed to the best fit values found in the non-flaring spectrum, gave an improvement of the fit at 99.9% confidence level. On the other hand the addition of a power law at high energies did not improve the fit: the χ^2 decreases from 145 (for 119 d.o.f) to 144 (118 d.o.f.), which is clearly not significant. To study the variation of the power law intensity with respect to the non-flaring spectrum we fixed

the photon index fixed to the best fit value of 1.9 found in the non-flaring spectrum, and calculated the corresponding power-law normalization. We find an upper limit (at 90% confidence level) on the power-law unabsorbed 0.1–200 keV flux of 3.6×10^{-10} ergs cm^{-2} s^{-1} ($\sim 1\%$ of the unabsorbed 0.1–200 keV flux during the flare). Therefore we conclude that there is evidence that the hard component weakens during the flare, although the upper limit is still compatible with the best fit power-law normalization during the non-flaring emission.

We report in Table 1 the best fit parameters corresponding to the spectra during the non-flaring and the flaring intervals. These spectra are shown in Figure 3 (top panels, a and b respectively), together with the residuals with respect to the best fit models (bottom panels). The unfolded spectra are also shown in Figure 4 (a and b, respectively), together with the components of the best fit models reported in Table 1.

3. Discussion

We fitted the BeppoSAX energy spectra of GX 349+2, extracted at different positions of the source in the CD. The best fit model up to energies of ~ 30 keV consists of a blackbody and a Comptonization spectrum (described by the `comptt` model), two emission lines and an absorption edge. The blackbody is at a temperature $kT_{\rm BB} \sim 0.5 - 0.6$ keV, and the radius of the blackbody (spherical) emitting region is $R_{\rm BB} \sim 35$ km (using a distance of 5 kpc, Cooke & Ponman 1991; Christian & Swank 1997). The temperature of the soft seed photons for the Comptonization is $kT_{\rm W} \sim 1$ keV. These are Comptonized in a hotter ($kT_{\rm e} \sim 3$ keV) region of moderate optical depth ($\tau \sim 10 - 12$ for a spherical geometry). The radius of the region emitting the seed-photon Wien spectrum, calculated as in In 't Zand et al. (1999), is $R_{\rm W} = 3 \times 10^4 D \sqrt{f_{bol}/(1+y)}/(kT_W)^2$ km $\sim 7 - 9$ km, where D is the distance in kpc, f_{bol} is the bolometric flux in ergs cm^{-2} s^{-1}, and kT_W is in keV. A broad (~ 0.7 keV FWHM) iron Kα emission line is present at ~ 6.7 keV, with equivalent width $\sim 30 - 70$ eV, accompanied by an absorption edge at ~ 8.5 keV. The high energy of both the line and edge indicates that these features are produced in a highly ionized region (corresponding approximately to Fe XXV). We also found evidence for an emission line at ~ 1.2 keV, with equivalent width of ~ 20 eV, which can be associated with emission from the L-shell of Fe XXIV or, perhaps, the K-shell of Ne X (see e.g. Kallman et al. 1996). We note that the main differences in the continuum below 30 keV between the spectra during the flares and the non-flaring emission are in the temperatures of the blackbody and Comptonized components: both temperatures are higher during the flares than during the non-flaring emission, while the optical depth of the Comptonized component is smaller during the flares. The iron emission line remains approximately unchanged.

A hard component is required to match the spectrum above 30 keV during the non-flaring emission. This component can be fit by a power-law with photon index ~ 2, contributing $\sim 2\%$ of the 0.1–200 keV source flux. This component is not required in the flare spectrum, where it probably weakens contributing a smaller fraction of the source flux. Evidence for such a hard component was previously found in this source by the *Ariel V* satellite (Greenhill et al. 1979), and

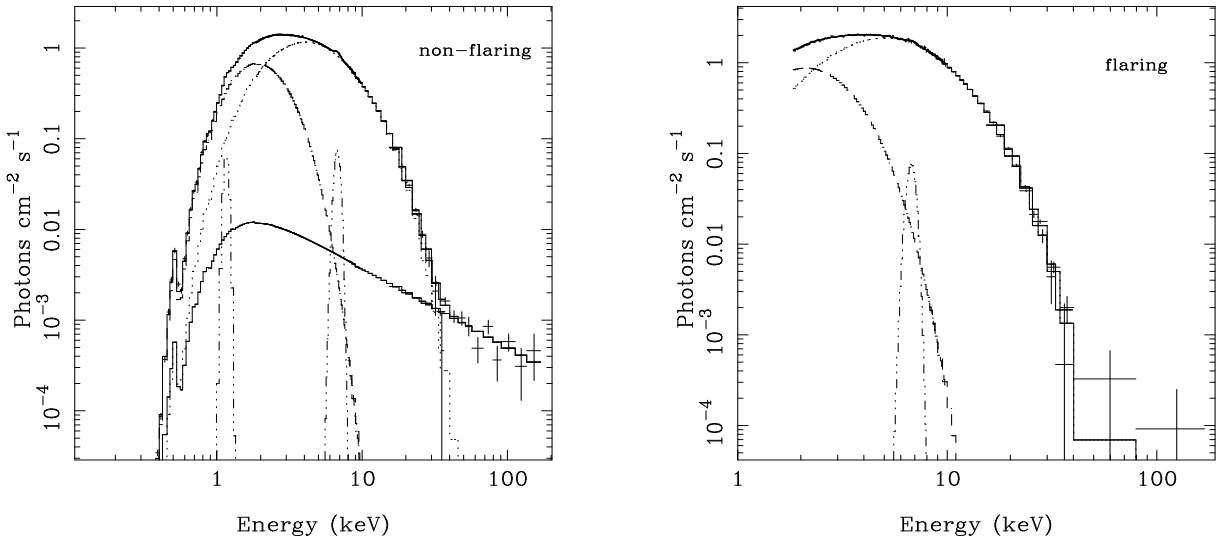

Fig. 4.— a) Unfolded spectrum of the GX 349+2 non-flaring emission and the best fit model of Table 1, shown in this figure as the solid line on top of the data. The individual model components are also shown, namely the blackbody (dashed line), the Comptonized spectrum (`comptt` model, dotted line), two Gaussian emission lines at ~ 1.2 keV and ~ 6.7 keV (dot-dot-dot-dashed lines), and the power-law (solid line). b) Unfolded spectrum of the GX 349+2 flaring emission and the best fit model of Table 1, shown as the solid line on top of the data. The components of the model are also shown, namely the blackbody (dashed line), the `comptt` model, (dotted line), and a Gaussian emission lines at ~ 6.7 keV (dot-dot-dot-dashed line).

was fit by a thermal spectrum with $kT \sim 30$ keV. In our data this component is much harder, corresponding to a temperature of ~ 120 keV. We note that the high energy instrument on board *Ariel V* had a field of view of 8° FWHM, much larger than the PDS field of view.

The smaller PDS field of view, 1.3° FWHM, reduces the possibility of the presence of contaminating sources. The eclipsing binary system 4U 1700–37 (the only nearby X-ray source brighter than 1 μJy, e.g. Valinia & Marshall 1998), is 1.4° away from GX 349+2, and out of the PDS field of view. Another possible contaminating source is the hard diffuse emission of the Galactic ridge. Using data from Valinia & Marshall (1998), for latitudes $1.5° < |b| < 4°$ and longitudes $|l| < 15°$ (the region of GX 349+2) the flux of the diffuse Galactic emission is $\sim 3.2 \times 10^{-11}$ ergs cm^{-2} s^{-1}

in the 10–60 keV energy range for the effective solid angle of the PDS FOV. This is one order of magnitude lower than the flux of the hard power-law component we detected from GX 349+2 in the same energy range. Given the flux of the power-law component in the 13–80 keV energy range, which is $\sim 1.2 \times 10^{-10}$ ergs cm^{-2} s^{-1}, we calculated the probability to find an active galactic nucleus in the PDS FOV at a flux level equal or higher than $\sim 1.2 \times 10^{-10}$ ergs cm^{-2} s^{-1}. We find a small probability of $\sim 2 \times 10^{-3}$ (see Fiore & Tamburelli 2000, in preparation; Levine et al. 1984). We can also exclude that this hard component is an instrumental feature, because in other BeppoSAX observations of soft sources there was no evidence of a hard excess. A clear example of this is given by the BeppoSAX spectrum of GX 17+2 in the lower NB (Di Salvo et al. 2000). We find that a power law with photon index 1.9, like that detected in this paper, is incompatible with those data, which give a 90% upper limit on the power-law unabsorbed 0.1–200 keV flux of 2.5×10^{-11} ergs cm^{-2} s^{-1}. It therefore is plausible that this hard component represents emission from GX 349+2.

A similar hard component has also been observed in other Z sources, indicating that this is probably a common feature of these sources. The presence (or strength) of these components appears to be related to the source state or its position in the CD. In a *Ginga* (1.5–38 keV energy range) observation of GX 5–1 a hard excess was detected (Asai et al. 1994).[6] This component was fit by a power law with photon index 1.8 (Asai et al. 1994), and its intensity decreased from the NB to the FB, *i.e.* from low to high mass accretion rate. In a BeppoSAX observation of GX 17+2 the hard component (power-law photon index of ~ 2.7) was detected in the HB and its intensity significantly decreased in the NB (Di Salvo et al. 2000). Cir X–1, thought to be a peculiar Z source (Shirey et al. 1998), was observed by BeppoSAX in the FB (Iaria et al. 2001). Also in this case a hard tail was detected in the non-flaring spectrum. We note that hard component detected here in GX 349+2 is one of the hardest among the high energy components detected so far in bright LMXBs. It corresponds to a photon index of ~ 1.9, with no evidence of a high energy cutoff in the BeppoSAX range. In fact, using thermal models to fit it, we obtain electron temperatures $\gtrsim 100$ keV. The power-law tail observed in the NB of GX 5–1 (Asai et al. 1994), had a photon index of ~ 1.8, similar to that we measured for GX 349+2. Also, Cir X–1 showed a spectral state similar to that of GX 349+2 observed here (Iaria et al. 2001). However, in Cir X–1 the power law was much steeper (photon index ~ 3.3) than in the case of GX 349+2, and the low energy continuum was characterized by a softer electron temperature of the Comptonized component $\lesssim 1$ keV. In all these cases the hard component seems to become weaker for higher accretion rates (see also Fig. 5), while the relative contribution of the hard component to the flux in a given source state appears to be different in different sources. Yet, in recent HEXTE observations of Sco X–1, a hard power-law tail was detected in 5 out of 16 observations, without any clear correlation with the position in the CD (D'Amico et al. 2000).

[6]Note, however, that the detection of a hard tail from GX 5–1 was not confirmed by SIGMA observations (Barret & Vedrenne 1994).

It is already known that some Atoll sources, the so-called X-ray bursters, can show a hard component in their spectra, similar to the observed spectra of accreting Black Holes (BH). Given that BHs and NSs are hardly distinguishable by their broad band spectral shape (see also Barret et al. 2000, and references therein), Barret et al. (1996) introduced another criterion based on the comparison of hard and soft luminosities. Plotting the 1–20 keV luminosity versus the 20–200 keV luminosity for BHs and NSs of the Atoll class, they observed that all NS systems in which a hard component had been detected lie in the so-called X-ray burster box, while all BH systems lie outside (see Fig. 5). If we plot in the same diagram the luminosities of the Z sources GX 17+2 (Di Salvo et al. 2000), Cir X–1 (Iaria et al. 2001), and GX 349+2 we find that these data lie clearly outside the X-ray burster box, and there is no clear distinction between Z sources and BHs (Fig. 5). Stated differently, this result shows that BHs are not the only sources to posses high energy tails when their 1–20 keV luminosity exceeds $\sim 1.5 \times 10^{37}$ ergs/s. In particular, the hard components in Z sources seem to be similar to the extended power-law tails detected in the so-called very-high state (and perhaps intermediate state) of Galactic BH systems (e.g. Grove et al. 1998). On the other hand it appears to be still true that only BHs can emit bright hard X-ray tails, with a 20–200 keV luminosity $\gtrsim 1.5 \times 10^{37}$ erg/s. This might be related to the higher Eddington luminosity that on average characterizes BHs. The fact that the luminosity in the hard tail observed in Z sources is similar in terms of Eddington luminosity to that seen in BHs is a further evidence that probably the same mechanism originates the hard tails in both BHs and NSs. This would imply that this mechanism does not depend on the presence or absence of a solid surface.

As in BHs, the hard tails observed in Z sources can be produced either in a thermal or non-thermal corona (e.g. Poutanen & Coppi 1998) or in a bulk motion of matter close to the NS (e.g. Titarchuk & Zannias 1998; Papathanassiou & Psaltis 2001). Fast radial converging motions are unlikely to be dominant in the innermost region of the accretion flow in such high-luminosity systems, because of the strong radiation pressure emitted from or close to the NS surface. However, power-law tails, dominating the spectra at high energy, can also be produced when the flows are mildly relativistic ($v/c \sim 0.1$) or when the velocity field does not converge (Psaltis 2001). Therefore azimuthal motions around the NS or outflows can be the probable origin of these components, with flatter power laws corresponding to higher optical depth of the scattering medium and/or higher bulk electrons velocities, in a way that is similar to thermal Comptonization (see Psaltis 2001). It has been proposed that non-thermal, high energy electrons, responsible for the hard tails observed in Z sources, might originate in a jet (Di Salvo et al. 2000, Iaria et al. 2001; see also Fender 2001 for a review regarding both BH and NS systems). In fact all the Z sources are detected as variable radio sources, with the highest radio fluxes associated with the HB. The radio emission weakens in the NB, and is not detected any longer in the FB (Hjellming & Han 1995, Fender & Hendry 2000, and references therein). This hypothesis is in agreement with the behavior of GX 17+2, where the hard tail was observed in the HB. In GX 349+2 the hard tail is present at the NB/FB vertex, where the radio flux should be near its minimum, and probably weakens when the source moves further into the FB. However, note that a similar correlation was not observed in the case of Sco X–1 (D'Amico et al. 2000). Further observations will help clarifying the correlation between hard

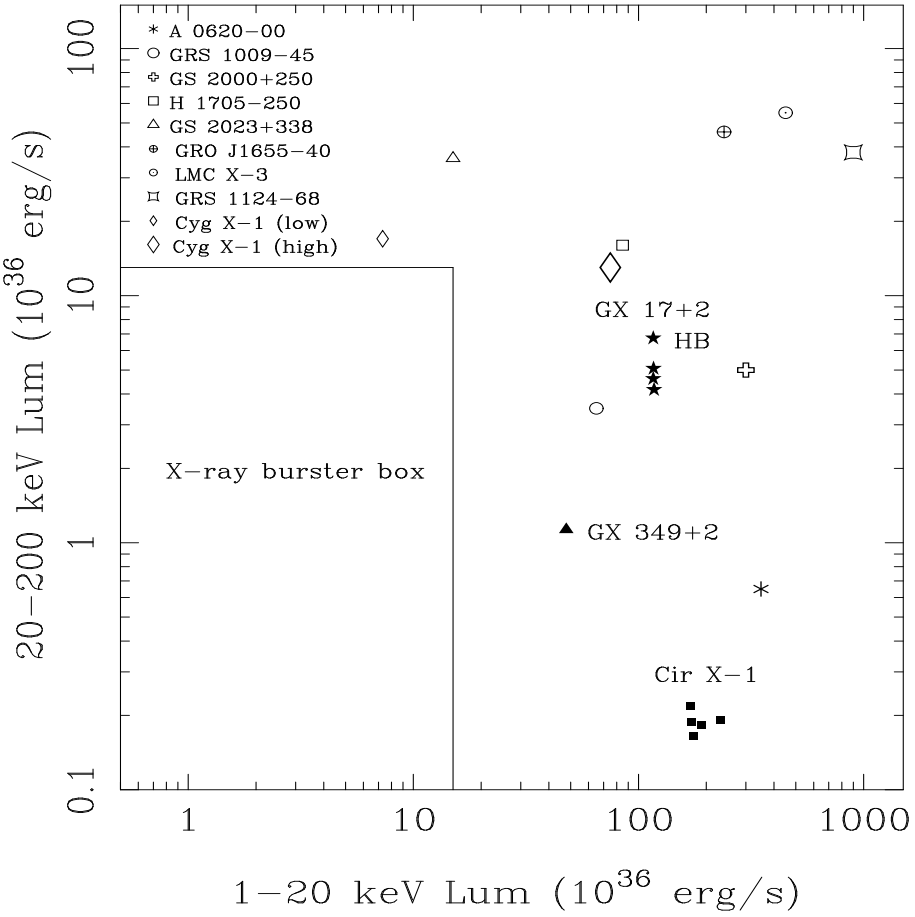

Fig. 5.— 20-200 keV versus 1-20 keV luminosities of BH binaries (open symbols, from Barret et al. 2000) and NS type-Z binaries (filled symbols). The so-called *X-ray burster box* is plotted as a solid line. Its boundaries are defined as in Barret et al. (2000).

X-ray and radio emission in these sources.

The authors thank D. Barret and L. Titarchuk for interesting discussions. This work was supported by the Italian Space Agency (ASI), by the Ministero della Ricerca Scientifica e Tecnologica (MURST).

REFERENCES

Agrawal, P. C., et al., 1971, Ap&SS, 10, 500

Asai, K., et al., 1994, PASJ, 46, 479

Barret, D., McClintock, J. E., Grindlay, J. E., 1996, ApJ, 473, 963

Barret, D., Olive, J. F., Boirin, L., Done, C., Skinner, G. K., Grindlay, J. E., 2000, ApJ, 533, 329

Barret, D., & Vedrenne, G., 1994, ApJS, 92, 505

Boella, G., Butler, R. C., Perola, G. C., Piro, L., Scarsi, L., Blecker, J., 1997a, A&AS, 122, 299

Boella, G., et al., 1997b, A&AS, 122, 327

Buselli, G., Clancy, M. C., Davison, P. J. N., Edwards, P. J., McCracken, K. C., Thomas, R. M., 1968, Nature, 219, 1124

Christian, D. J., & Swank, J. H., 1997, ApJS, 109, 177

Cooke, B. A., Ponman, T. J., 1991, A&A, 244, 358

D'Amico, F., Heindl, W. A., Rothschild, R. E., Gruber, D. E., ApJL, submitted (astro-ph/0008279)

Di Salvo, T., et al., 2000, ApJL, 544, in press

Fender, R. P., 2001, Proc. International Symposium on High Energy Gamma-Ray Astronomy, Heidelberg, Eds. F. Aharonian & H. Voelk, AIP, in press (astro-ph/0101233)

Fender, R. P., & Hendry, M. A., 2000, MNRAS, 317, 1

Frontera, F., et al., 1997, A&AS, 122, 357

Greenhill, J. G., Coe, M. J., Burnell, S. J. B., Strong, K. T., Carpenter, G. F., 1979, MNRAS, 189, 563

Grove, J. E., Johnson, W. N., Kroeger, R. A., McNaron-Brown, K., Skibo, J. G., Phlips, B. F., 1998, ApJ, 500, 899

Hasinger, G., & van der Klis, M., 1989, A&A, 225, 79

Hasinger, G., van der Klis, M., Ebisawa, K., Dotani, T., Mitsuda, K., 1990, A&A, 235, 131

Haymes, R. C., Harnden, F. R., Johnson, W. N., Prichard, H. M., Bosch, H. E., 1972, ApJ, 172, L47

Hjellming, R. M., & Han, X. H., 1995, in *X-ray Binaries*, , Lewin W. H. G., van Paradijs J., van den Heuvel E. P. J. eds., Cambridge Astrophysics Series, 308

Iaria, R., Burderi, L., Di Salvo, T., La Barbera, A., Robba, N. R., 2001, ApJ, 547, in press (astro-ph/0009183)

In't Zand, J. J. M., et al., 1999, A&A, 345, 100

Jain, A., et al., 1984, A&A, 140, 179

Kallman, T. R., Liedahl, D., Osterheld, A., Goldstein, W., Kahn, S., 1996, ApJ, 465, 994

Levine, A. M., et al., 1984, ApJS, 54, 581

Magdziarz, P., & Zdziarski, A. A., 1995, MNRAS, 273, 837

Manzo, G., Giarrusso, S., Santangelo, A., Ciralli, F., Fazio, G., Piraino, S., Segreto, A., 1997, A&AS, 122, 341 Masetti, N., et al., 2000, A&A, in press (astro-ph/0009044)

Mitsuda, K., et al., 1984, PASJ, 36, 741

Miyamoto, S., & Matsuoka, M., 1977, SSRv, 20, 687

Nishimura, J., Mitsuda, K., Itoh, M., 1986, PASJ, 38, 819

Papathanassiou, H., & Psaltis, D., 2001, MNRAS, in press (astro-ph/0011447)

Parmar, A. N., et al., 1997, A&AS, 122, 309

Peterson, L. E., & Jacobson, A. S., 1966, ApJ, 145, 962

Poutanen, J., & Coppi, P. S., 1998, Phys. Scripta, T77, 57

Psaltis, D., 2001, ApJ, in press (astro-ph/0011534)

Riegler, G. R., Boldt, E., & Serlemitsos, P., 1970, Nature, 266, 1041

Shirey, R. E., Bradt, H. V., Levine, A. M., Morgan, E. H., 1998, ApJ, 506, 374

Soong, Y., Rothschild, R. E., 1983, ApJ, 274, 327

Strickman, M., & Barret, D., Detections of multiple hard X-ray flares from Sco X-1 with OSSE, in AIP Conf. Proc. 510, Proc. of the Fifth Compton Symposium, Eds M.L. McConnel and J.M. Ryan (New York:AIP), 222-226, 2000

Sunyaev, R. A., Titarchuk, L. G., 1980, A&A, 86, 121

Titarchuk, L., 1994, ApJ, 434, 570

Titarchuk, L., & Zannias, T., 1998, ApJ, 493, 863

Ubertini, P., Bazzano, A., Cocchi, M., La Padula, C., Sood, R. K., 1992, ApJ, 386, 710

Valinia, A., & Marshall, F. E., 1998, ApJ, 505, 134

Zhang, W., Strohmayer, T. E., Swank, J. H., 1998, ApJ, 500, L167

TABLES

Table 1: Results of the fitting of the GX 349+2 spectra in the 0.12–200 keV energy band. The model consists of a blackbody, a Comptonized spectrum modeled by `comptt`, a power law, two Gaussian emission lines, and an absorption edge. Uncertainties are 90% confidence level for a single parameter of interest. The power-law normalization is in units of ph keV^{-1} cm^{-2} s^{-1} at 1 keV. The total unabsorbed flux is in the 0.1–200 keV energy range. The effective exposure time was a factor of ~ 20 larger in the non-flaring spectrum than in the flaring.

Parameter	Non-Flaring	Flare
$N_{\rm H}$ ($\times 10^{22}$ cm^{-2})	$0.66^{+0.03}_{-0.02}$	0.64 ± 0.3
$kT_{\rm BB}$ (keV)	0.51 ± 0.01	0.59 ± 0.02
$R_{\rm BB}$ (km)	36 ± 2	31 ± 2
$kT_{\rm W}$ (keV)	1.03 ± 0.03	1.37 ± 0.04
$kT_{\rm e}$ (keV)	2.65 ± 0.05	2.95 ± 0.07
τ	11.7 ± 0.4	10.5 ± 0.5
$R_{\rm W}$ (km)	8.8 ± 0.6	7.0 ± 0.5
Photon Index	$1.9^{+0.4}_{-0.3}$	1.9 (fixed)
Power-law N	$3^{+9}_{-2} \times 10^{-2}$	$< 2.3 \times 10^{-2}$
$E_{\rm Fe}$ (keV)	6.73 ± 0.05	6.73 (fixed)
$\sigma_{\rm Fe}$ (keV)	0.31 ± 0.08	0.31 (fixed)
$I_{\rm Fe}$ ($\times 10^{-3}$ ph cm^{-2} s^{-1})	8.8 ± 1.5	8.5 ± 3.7
Fe Eq. Width (eV)	71	34
$E_{\rm LE}$ (keV)	1.16 ± 0.03	–
$\sigma_{\rm LE}$ (keV)	0.05 ± 0.05	–
$I_{\rm LE}$ ($\times 10^{-2}$ ph cm^{-2} s^{-1})	$1.9^{+0.8}_{-0.5}$	–
LE Eq. Width (eV)	17	–
$E_{\rm edge}$ (keV)	8.9 ± 0.2	–
$\tau_{\rm edge}$ ($\times 10^{-2}$)	4 ± 1	–
Flux (ergs cm^{-2} s^{-1})	1.91×10^{-8}	3.26×10^{-8}
χ^2_{red} (d.o.f.)	1.17 (189)	1.22 (119)